Spatial Distribution of Competing Ions around DNA in Solution

K. Andresen,[1] R. Das,[2,3] H. Y. Park,[1] H. Smith,[1] L. W. Kwok,[1] J. S. Lamb,[1] E. J. Kirkland,[1] D. Herschlag,[3,4] K. D. Finkelstein,[5] and L. Pollack[1]

[1]*School of Applied and Engineering Physics, Cornell University, Ithaca, New York 14853, USA*
[2]*Department of Physics, Stanford University, Stanford, California 94305, USA*
[3]*Department of Biochemistry, Stanford University, Stanford, California 94305, USA*
[4]*Department of Chemistry, Stanford University, Stanford, California 94305, USA*
[5]*Cornell High Energy Synchrotron Source (CHESS), Cornell University, Ithaca, New York 14853, USA*

(Received 7 June 2004; published 7 December 2004)

The competition of monovalent and divalent cations for proximity to negatively charged DNA is of biological importance and can provide strong constraints for theoretical treatments of polyelectrolytes. Resonant x-ray scattering experiments have allowed us to monitor the number and distribution of each cation in a mixed ion cloud around DNA. These measurements provide experimental evidence to support a general theoretical prediction: the normalized distribution of each ion around polyelectrolytes remains constant when ions are mixed at different ratios. In addition, the amplitudes of the scattering signals throughout the competition provide a measurement of the surface concentration parameter that predicts the competition behavior of these cations. The data suggest that ion size needs to be taken into account in applying Poisson-Boltzmann treatments to polyelectrolytes such as DNA.

DOI: 10.1103/PhysRevLett.93.248103 PACS numbers: 87.14.Gg, 61.10.Eq, 87.15.–v

The conformation of DNA and its packing into cellular and viral compartments play critical roles in the transmission and expression of genetic information in living systems [1]. Integral to DNA's structure and function are its interactions with multiple metal ions, organic cations, and cationic proteins [2]. These interactions occur within a diffuse background of ions that surround DNA. The fundamental behavior of DNA cannot be understood without accounting for this counterion atmosphere and the competition between different cations for inclusion within it.

The strong salt dependences of folding and intermolecular interactions of nucleic acids and of synthetic polyelectrolytes [3] underscore the need for accurate modeling of the counterion distributions. Interactions with counterions are also critical in facilitating attractive forces between negatively charged strands, such as those driving DNA condensation [4–6] and actin bundle formation [7,8]. Furthermore, the interpretation of electrophoretic mobilities and other transport properties relies on an accurate treatment of the ion atmosphere [9].

Early treatments of the interaction of DNA with oppositely charged particles began in the 1970s with Manning's counterion condensation theory [10]. Although this model accurately predicts many experimental results [11], it makes no specific predictions of the spatial distribution of ions around the DNA. Functional forms of the distributions rely on models based on application of the Poisson-Boltzmann (PB) equation [12]. Although simplifying assumptions within the PB treatment limit its applicability [13], this model is in agreement with experimental data reflecting the positions of monovalent ions or divalent ions around DNA [14–16].

In biological systems, the solution around DNA is composed of multiple cationic species. For these mixed-valence solutions, and in nearly all experimental systems, the question of preferential binding arises. A qualitative analysis of entropy suggests that the localization of a single divalent ion would be favored over the localization of two monovalent ions required to neutralize the same amount of charge [17]. Previous measurements of ionic competition by magnetic resonance relaxation times [12], electrophoresis [18], and equilibrium dialysis [19] strongly support this preference. These techniques can distinguish bound from unbound charges but they do not provide the critical information about how these ions are distributed in space. Thus, quantitative comparison to experiment has required an untested assumption that the spatial distribution of an ion remains constant as its concentration is lowered by competition with another ion [20].

We previously demonstrated that anomalous (resonant) small angle x-ray scattering (ASAXS) can be used to obtain quantitative information about the distribution of ions. The distributions of a monovalent ion, Rb^+, and of a divalent ion, Sr^{2+}, around a DNA duplex were shown to be consistent with predictions for distributions of single cations from PB theory [15]. Herein we report ASAXS experiments of ion competition that provide more stringent tests of the accuracy and applicability of PB treatments. The critical assumption that the spatial distribution of an ion is constant when in competition with another ion has now been tested and shown to hold. Further, these results allow determination of a critical surface concentration parameter that allows the prediction of competition behavior of monovalent and divalent cations. However, the derived concentration parameter

does not appear to be accounted for by the simplest PB treatments in which ions are treated as point charges. This discrepancy can be resolved if the finite size of the ions is considered.

Small angle x-ray scattering probes the size, shape, and compactness of molecules in solution. The scattering of x rays by molecules results from spatial variations in electron density in the sample [21]. The electron density of the DNA-counterion system has three components: the DNA, the bulk solution far from the DNA, and the high concentration, territorially bound layer [inset Fig. 1(a)].

Scattering from the ions can be selectively probed using ASAXS [22]. In these experiments, the energy of the incident x ray is tuned to approach the energy to eject an electron from an inner atomic shell. Far from this atomic resonance, or edge, the scattering power of an isolated atom, f_0, is proportional to atomic number. Just below the edge, the real part of the scattering power is reduced by the real part of the anomalous scattering factor f' [23,24]. The imaginary part of the scattering factor, the photoelectric absorption f'', is modest [22]. To

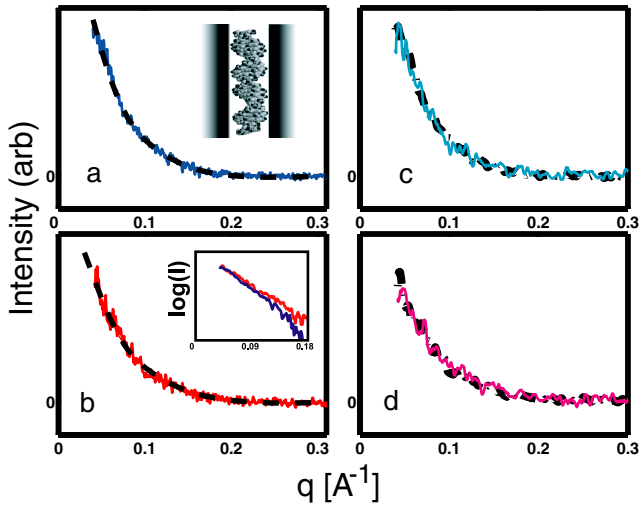

FIG. 1 (color online). In part (a), the measured anomalous signal for monovalent rubidium ions in Rb-DNA is shown. The smooth, dashed curve is the best fit to the analytical theory described in the text. The inset shows a cartoon of the sample and indicates density variations of the counterions by shading. Part (b) shows measured and predicted curves for divalent Sr^{2+} ions in Sr-DNA. The inset illustrates the difference in the shape of the anomalous signals for monovalent ions (lower, blue curve) and divalent ions (upper, red curve). The tighter spatial localization of divalent ions is reflected by the higher intensity at larger scattering angle. In parts (c) and (d) anomalous signals for both types of ions are shown in two different bulk solutions. The curve amplitudes have been scaled to illustrate the shape similarity under different solution conditions. In (c), the darker (black) curve was acquired in a pure rubidium solution (0.1 M Rb^+); the lighter (cyan) curve was acquired in 0.09 M Rb^+ and 0.01 M Sr^{2+}. In (d), the darker (black) curve was acquired in an all strontium solution (0.1 M Sr^{2+}). The lighter (magenta) curve was acquired in 0.09 M Rb^+, 0.01 M Sr^{2+}.

carry out these experiments, SAXS profiles are acquired at two energies: one just below the absorption edge and the second 0.1 keV lower in energy, where resonant effects can be ignored. We refer to these energies as "on-edge" and "off-edge," respectively. Subtraction of these two profiles, appropriately normalized, yields a signal that reports on the spatial distribution of the resonant element, in this case the counterions.

The DNA samples were purchased from Integrated DNA Technologies. The sequence and sample preparation were described in Ref. [15]. Duplex DNA was dialyzed against a series of salt solutions, with composition ranging from pure monovalent cation, 0.1 M rubidium acetate, to pure divalent cation, 0.1 M strontium acetate. Following dialysis, the DNA concentration was adjusted to 0.2 mM, as determined by absorbance at 260 nm.

SAXS data were collected at the Cornell High Energy Synchrotron Source (CHESS) C1 bend magnet station, where high intensity, tunable x-rays (bandwidth 4–5 eV at 16 keV) are available [25]. Monovalent ions, (Rb^+), were probed using x-rays of 15.098 and 15.198 keV. Divalent ions, (Sr^{2+}), were probed at 16.008 and 16.108 keV. The 3 mm path length, low volume (50 μL) sample cells use ultrathin silicon nitride films, fabricated at the Cornell Nanoscale Science and Technology Facility (CNF), as x-ray windows. Each scattering profile was normalized to the transmitted intensity over the 30-second exposure. At each energy, the intensity $I(q)$ was determined by subtracting a DNA absent background profile from the DNA present signal profile. The anomalous difference results by subtracting on-edge profiles from off-edge profiles.

To predict the shape of the anomalous signal for comparison to the data, the angular distribution of x-ray scattering intensity from the DNA-ion sample was computed. For a multicomponent system, the form factor $\sum f_i F_i(q)$ (where f_i is the scattering factor of component i relative to a background and $F_i(q)$ reflects the spatial distribution of component i [26,27]) was calculated and multiplied by its complex conjugate [27]. For this system

$$I(q) = [f_{\mathrm{DNA}}F_{\mathrm{DNA}}(q) + f_{\mathrm{ion}}F_{\mathrm{ion}}(q)][f_{\mathrm{DNA}}F_{\mathrm{DNA}}(q) + f_{\mathrm{ion}}F_{\mathrm{ion}}(q)]^{\star}, \quad (1)$$

where $q = 4\pi \sin\theta/\lambda$, θ is half the scattering angle, and λ is the x-ray wavelength. Close to an atomic resonance $f_{\mathrm{ion}} = [f_0 + f'(E) + \imath f''(E)]$ [28]. The intensity was calculated at two energies and the anomalous difference signal was extracted by subtracting the on-edge from off-edge prediction. The functional form for the anomalous difference signal can be derived from Eq. (1), recognizing that subtraction removes energy independent terms

$$I_{\mathrm{anom}}(q) = 2\alpha F_{\mathrm{DNA}}(q)F_{\mathrm{ion}}(q) \times f_{\mathrm{DNA}}[f'_{\mathrm{ion}}(E_{\mathrm{on}}) - f'_{\mathrm{ion}}(E_{\mathrm{off}})] \quad (2)$$

where α is the constant of proportionality between the

measured signal and number of scattered x rays. The small ion-ion term has been neglected, as have the small effects from the anion distributions [15].

Figure 1 shows representative data for the DNA duplex in Rb^+ alone, in Sr^{2+} alone, and in a mixture of the two ions. Both analytical and numerical solutions have been employed to evaluate Eq. (2) for comparison to the data. In the analytical approach, outlined in Ref. [28], the DNA was modeled as a finite-length cylinder of radius 1 nm and the excess ion concentration, $\Delta n(r)$, was solved for [20]; the excess concentration profile is used because SAXS is sensitive to electron density differences relative to the bulk solvent. Good agreement between the data in Rb^+ or Sr^{2+} alone and the model is observed [Figs. 1(a) and 1(b)]. Fits of comparable quality are obtained from numerical solutions with atomic models of DNA and were published previously [15].

As noted above, PB theory predicts the normalized spatial distribution of a given ion to be invariant as bulk salt concentration changes (up to ~0.4 M), even as the ion number decreases due to competition ([16,20,29,30] and calculations not shown). We have tested this prediction by comparing the shape of anomalous signals under mixed salt conditions to those acquired in pure monovalent and pure divalent solutions. The representative results in Figs. 1(c) and 1(d) show that the normalized scattering profile for each species is independent, within error, of the makeup of the bulk solution. Analogous results were obtained for four other mixed Rb^+/Sr^{2+} solutions within noise (data not shown).

Although the shape of the ion distribution is constant, the amount in the ion cloud is decreased by competition with the other ion. The number of each ion in the ion cloud can be predicted from standard PB electrostatic treatments of charged surfaces if an appropriate surface concentration parameter is known (see below). Our measurements allow a quantitative determination of this concentration parameter.

The PB theory requires a simple relation [20,29] between the surface and bulk concentrations, N_{s_i} and N_{b_i}, of any ionic species: $N_{s_i} = N_{b_i} e^{z\Psi_s}$, where Ψ_s is the reduced surface potential [20] and z is the ion valence. In terms of reduced surface concentrations, $n_{s_1}(n_{s_2})$ corresponding to $N_{s_1}(N_{s_2})$ normalized to $N_{s_1}^{\max}(N_{s_2}^{\max})$, measured in pure monovalent (divalent) solution, application of the Boltzmann equation leads to [20]:

$$\frac{n_{s_2}}{n_{s_1}^2} = \frac{N_{b_2}}{N_{b_1}^2} \frac{N_{s_1}^{\max 2}}{N_{s_2}^{\max}}. \quad (3)$$

The ratio on the left side of this equation is measured and is related to the (known) bulk concentrations by a single concentration parameter, $N_{s_1}^{\max 2}/N_{s_2}^{\max}$. From Eq. (2) and the functional form for $\Delta n(r)$ from Ref. [20], it follows that $I_{\text{anom}}(q)$ is directly proportional to the surface concentration, N_{s_i}, of an ion. The ASAXS measurements therefore allow the determination of the n_{s_i} values, a test of the relationship in Eq. (3), and extraction of the critical parameter, $N_{s_1}^{\max 2}/N_{s_2}^{\max}$.

Measurements of the anomalous difference signals of the monovalent ion, Rb^+, and the divalent ion, Sr^{2+} were carried out in seven different solutions, ranging from pure Rb^+ to pure Sr^{2+}, while maintaining a constant total cation concentration of 0.1 M. Values of $N_{s_1} = N_{s_{Rb}}$ and $N_{s_2} = N_{s_{Sr}}$ were determined for each ion type (up to a scale factor) by fitting the scattering profile to Eq. (2). To use Eq. (3), the reduced surface concentrations, n_{s_1} and n_{s_2} were obtained by normalizing the best-fit coefficient for each measured anomalous signal to the coefficient obtained in the limiting case, when the solution consists of that ion alone. All 14 data points are plotted in Fig. 2 as a function of the concentration of Sr^{2+} in bulk solution. The reduced surface concentrations sum to unity within error, a boundary condition expected from numerical solutions to the PB model [29] (Fig. 2, inset).

The solid lines shown in Fig. 2 represent the best fit of Eq. (3) to all of the data points. We find a good fit to the data, providing support for the ability of PB treatments to describe the electrostatics underlying ion competition. Nevertheless, the best-fit value of $N_{s_1}^{\max 2}/N_{s_2}^{\max} = 2.1 \pm 0.2$ M is smaller than the value 2.9 M expected from the standard treatment of DNA where it is modeled as a uniformly charged cylinder [12]. The better agreement of the former value (2.1 M) than the latter value (2.9 M) is evident by comparison of the χ^2 values, 1.4 and 2.6, respectively. The discrepancy between our measured

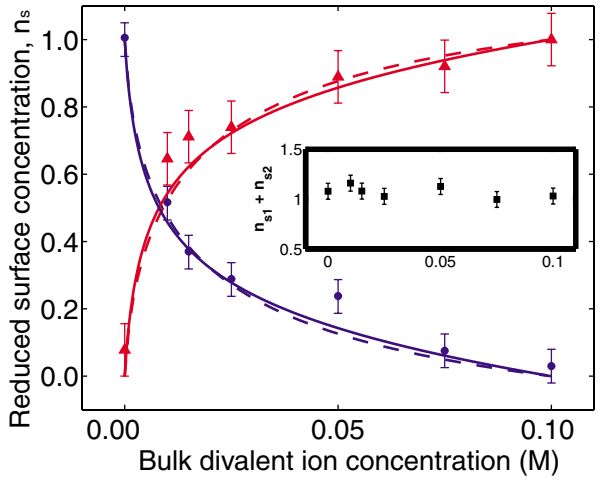

FIG. 2 (color online). The measured reduced surface concentrations of Rb^+ (solid blue circles) and Sr^{2+} (solid red triangles) ions are shown as the bulk solution composition is varied. The solid lines represent the best fit of Eq. (3) to the data. The dashed lines represent the predictions of numerical calculations with finite ionic radius, i.e., the distance of closest approach of both types of ions to the DNA. A curve corresponding to a representative value of 2 Å is shown. Both approaches result in good agreement with the data. The inset shows that the sum of the reduced surface concentrations equals unity (solid line), within error.

value and the expected value can be accounted for if the finite sizes of the ions are taken into consideration. Size effects modify the surface concentration in two ways. First, each ion's closest approach to the DNA surface is determined by its hydrated radius (1–3 Å for Rb^+ and 1–4 Å for Sr^{2+} depending on the treatment of the ionic hydration shell [31]). Second, competition can also be influenced by differences in the ligand size [29]. Both of these effects reduce the expected surface concentration relative to the prediction for point charges, and bring the PB theory into agreement with the measurements. To further evaluate this hypothesis, we carried out numerical solutions of the PB equation with an atomic resolution model. The numbers of bound ions were derived from an integration of the excess ion profile calculated with Delphi [15,32] using a closest approach of 2–4 Å and give excellent agreement with the data (Fig. 2). In summary, both the analytic and numerical approaches result in excellent agreement with the data when finite ion size effects are included.

Using resonant scattering, we have distinguished the scattering profiles of two different species of ions competing in the charge neutralization of DNA. This method supports several basic predictions of PB theory: distributions of ions in competition are invariant in shape; the reduced surface concentrations of ions sum to unity; and the change in the number of bound ions throughout the competition follows a simple Boltzmann relationship, Eq. (3). Nevertheless, this agreement requires a surface concentration parameter smaller than that predicted from elementary electrostatic considerations. This difference likely results from ion size effects, which are not included in the simplest PB treatments. The measurement of the surface concentration parameter, coupled with the observed robustness of the spatial distribution of competing ions, provides critical information required for accurate modeling of ion distributions around charged surfaces.

We thank Vijay Pande for discussions and John Nagle and Ernie Fontes for assistance with the experiment. This research is funded by the NIH through P01-GM066275, the NSF through MCB-0347220 and the NBTC at Cornell, and NASA through NAG8-1778. CHESS is supported by the NSF and the NIH/NIGMS under Grant No. DMR-9713424. The CNF is supported by the NSF, Cornell University and industrial affiliates.

[1] B. Alberts *et al.*, *Molecular Biology of the Cell* (Garland Science, New York, 2002).
[2] L. McFail-Isom, C. C. Sines, and L. D. Williams, Curr. Opin. Struct. Biol. **9**, 298 (1999).
[3] F. J. Solis and M. Olvera de la Cruz, Eur. Phys. J. E **4**, 143 (2001).
[4] W. M. Gelbart, R. F. Bruinsma, P. A. Pincus, and V. A. Parsegian, Phys. Today **53**, No. 9, 38 (2000).
[5] A. Y. Grosberg, T. T. Nguyen, and B. I. Shklovskii, Rev. Mod. Phys. **74**, 329 (2002).
[6] J. C. Butler, T. Angelini, J. X. Tang, and G. C. L. Wong, Phys. Rev. Lett. **91**, 028301 (2003).
[7] T. E. Angelini *et al.*, Proc. Natl. Acad. Sci. U.S.A. **100**, 8634 (2003).
[8] G. C. L. Wong *et al.*, Phys. Rev. Lett. **91**, 018103 (2003).
[9] S. A. Allison, H. Wang, T. M. Laue, T. J. Wilson, and J. O. Wooll, Biophys. J. **76**, 2488 (1999).
[10] G. S. Manning, J. Chem. Phys. **51**, 924 (1969).
[11] C. F. Anderson and M. T. Record, Jr., Annu. Rev. Phys. Chem. **33**, 191 (1982).
[12] C. F. Anderson and M. T. Record, Jr., Annu. Rev. Biophys. Biophys. Chem. **19**, 423 (1990).
[13] J. Israelachvili, *Intermolecular and Surface Forces* (Acedemic Press, London, 1997).
[14] J. R. C. van der Maarel and K. Kassapidou, Macromolecules **31**, 5734 (1998).
[15] R. Das *et al.*, Phys. Rev. Lett. **90**, 188103 (2003).
[16] C. F. Wu, S. H. Chen, L. B. Shih, and J. S. Lin, Phys. Rev. Lett. **61**, 645 (1988).
[17] R. J. Bacquet and P. J. Rossky, J. Phys. Chem. **92**, 3604 (1988).
[18] A. Z. Li, H. Huang, X. Re, L. J. Qi, and K. A. Marx, Biophys. J. **74**, 964 (1998).
[19] W. H. Braunlin, T. J. Strick, and M. T. Record, Jr., Biopolymers **21**, 1301 (1982).
[20] I. Rouzina and V. A. Bloomfield, Biophys. Chem. **64**, 139 (1997).
[21] C. R. Cantor and P. R. Schimmel, *Biophysical Chemistry* (W. H. Freeman & Co., New York, 2001).
[22] A. Naudon, *Modern Aspects of Small-Angle Scattering*, edited by H. Brumberger (Kluwer Acedemic Publishers, Dordrecht/Boston/London, 1993).
[23] R. W. James, *The Optical Principles of the Diffraction of X-Rays* (OxBow Press, Woodbridge, CT, 1982).
[24] A. J. C. Wilson and E. Prince, *International Tables For Crystallography* (Kluwer Acedemic Publishers, Dordrecht/Boston, 1999).
[25] K. D. Finkelstein, P. M. Abbamonte, and V. O. Kostroun, Proc. SPIE Int. Soc. Opt. Eng. **4783**, 139 (2002).
[26] B. Guilleaume, J. Blaul, M. Wittemann, M. Rehahn, and M. Ballauff, J. Phys. Condens. Matter **12**, A245 (2000).
[27] S. L. Chang, S. H. Chen, R. L. Rill, and J. S. Lin, J. Phys. Chem. **94**, 8025 (1990).
[28] B. Guilleaume *et al.*, Colloid Polym. Sci. **279**, 829 (2001).
[29] I. Rouzina and V. A. Bloomfield, J. Phys. Chem. **100**, 4305 (1996).
[30] I. Rouzina and V. A. Bloomfield, J. Phys. Chem. **100**, 4292 (1996).
[31] B. E. Conway, *Ionic Hydration in Chemistry and Biophysics* (Elsevier Scientific Pub. Co., Amsterdam, 1981).
[32] S. W. W. Chen and B. Honig, J. Phys. Chem. B **101**, 9113 (1997).